On Model Robustness Against Adversarial Examples

Shufei Zhang
Department of Electrical and Electronic Engineering
Xi'an Jiaotong-Liverpool University
Shufei.Zhang@xjtlu.edu.cn

Kaizhu Huang
Department of Electrical and Electronic Engineering
Xi'an Jiaotong-Liverpool University
Kaizhu.Huang@xjtlu.edu.cn

Zenglin Xu
University of Electronic Science and Technology of China
zenglin@gmail.com

Abstract

We study the model robustness against adversarial examples, referred to as small perturbed input data that may however fool many state-of-the-art deep learning models. Unlike previous research, we establish a novel theory addressing the robustness issue from the perspective of stability of the loss function in the small neighborhood of natural examples. We propose to exploit an energy function to describe the stability and prove that reducing such energy guarantees the robustness against adversarial examples. We also show that the traditional training methods including adversarial training with the l_2 norm constraint (AT) and Virtual Adversarial Training (VAT) tend to minimize the lower bound of our proposed energy function. We make an analysis showing that minimization of such lower bound can however lead to insufficient robustness within the neighborhood around the input sample. Furthermore, we design a more rational method with the energy regularization which proves to achieve better robustness than previous methods. Through a series of experiments, we demonstrate the superiority of our model on both supervised tasks and semi-supervised tasks. In particular, our proposed adversarial framework achieves the best performance compared with previous adversarial training methods on benchmark datasets MNIST, CIFAR-10, and SVHN. Importantly, they demonstrate much better robustness against adversarial examples than all the other comparison methods.

Introduction

Deep Neural Networks (DNN) have achieved great success in various tasks, such as speech recognition, image classification, and object detection (LeCun, Bengio, and Hinton 2015; He et al. 2017). However, recent research shows that certain small perturbations over the input samples, called adversarial examples, may fool many powerful deep learning models (Goodfellow, Shlens, and Szegedy 2014).

To better handle the adversarial perturbation, there have been many seminal works studying how to generate adversarial examples. For example, Liu et al. presented a simple way called L-BFGS method to generate such examples (Liu and Nocedal 1989). Fast Gradient Sign Method (FGSM) was later proposed, which can also generate the adversarial perturbation (Goodfellow, Shlens, and Szegedy 2014). Lyu et al. and Shaham et al. further extended the FGSM to more general cases with the l_p norm constraint (Lyu, Huang, and Liang 2015; Shaham, Yamada, and Negahban 2015), where FGSM can be seen as the adversarial training method with l_∞ norm. Kurakin et al. attempted to utilize the projected gradient on the negative loss to find the worst perturbation called FGSM^k (Kurakin, Goodfellow, and Bengio 2016), which can be viewed as the multi-step version of FGSM. Focusing on studying the gradient of the loss function, these three methods showed their effectiveness in improving the model robustness on both natural and adversarial examples by data augmentation with adversarial examples.

On the other hand, for defending the adversarial attack, defensive distillation and feature squeezing were investigated (Xu, Evans, and Qi 2017; Papernot, McDaniel, and Goodfellow 2016). Furthermore, Virtual Adversarial Training (VAT) can generate adversarial perturbation without label information (Miyato et al. 2015; Miyato et al. 2018). More specifically, the objective of VAT is to smooth the output distribution by minimizing the divergence between outputs of natural examples and adversarial examples. In addition, Kos et al. proposed methods to generate the adversarial examples for generative models (Kos, Fischer, and Song 2018).

In parallel to studying how adversarial examples can be generated, researchers also made great efforts in thinking about the theory and principles underlying the adversarial examples. In particular, Ma et al. have shown that adversarial examples are not isolated points but a dense region of the input space (Ma et al. 2018). Fawzi et al. studied the model robustness against adversarial examples by establishing a general upper bound (Fawzi, Moosavi-Dezfooli, and Frossard 2016; Fawzi, Fawzi, and Frossard 2018). Finlay et al. and Lyu et al. have demonstrated that FGSM and their extended general cases can be interpreted as a form of regularization (Finlay, Oberman, and Abbasi 2018; Lyu, Huang, and Liang 2015). Similarly, Cisse et al. showed that the sensitivity to adversarial examples can be controlled by the Lipschitz constant of the network and proposed a new structure of network which is insensible to adversarial examples (Cisse et al. 2017).

The above-mentioned seminal studies have got interesting and important results for trying to understand adversarial examples. Although some theoretical robustness bounds have been proposed, most are practically difficult to be used or be optimized. Moreover, less theories have been rigorously offered on measuring the model robustness against adversarial examples mathematically and systematically.

Distinguished from these existing work, in this paper, a novel theoretical framework has been established which is able to address the robustness issue mathematically and rigorously.

In more details, inspired from the stability of the loss function in the small neighborhood of natural examples, we propose to exploit an energy function to describe the stability, and we prove that reducing such energy guarantees the robustness against adversarial examples. We also prove that many traditional adversarial training methods (including both supervised and semi-supervised adversarial training) are essentially equivalent to minimizing the lower bound of the proposed energy function; such low bound minimization can however might lead to insufficient robustness within the neighborhood around the input sample. Furthermore, we design a more rational and practical method with the energy regularization which proves to achieve better robustness than previous methods.

In addition, we develop the robustness analysis on both traditional supervised and semi-supervised adversarial learning, which is, to our best knowledge, rarely seen in the literature.

Finally, to verify the performance of the proposed method, we have conducted a series of experiments for both supervised and unsupervised tasks. Experimental results have shown that our proposed adversarial framework can achieve the best performance compared with previous adversarial methods benchmarked on MNIST, CIFAR-10, and SVHN. Importantly, they demonstrate much better robustness against adversarial examples than all the other comparison methods.

Notations and Backgrounds

We denote by D_{train} a training set containing N samples, namely $D_{train} = \{x_i, y_i | i = 1, ..., N\}$, where $x_i \in \mathbb{R}^I$ indicates an input sample (or natural sample) and $y_i \in \mathbb{R}^O$ denotes its corresponding label (with I and O representing the dimension of the input space and the output space, respectively). We also define $B(x_i, \epsilon)$ as an I-dimensional small ball around each x_i with the radius ϵ.

Given a specific type of DNN, we let $f(x, \theta) : R^I \rightarrow R^O$ denote its mapping function (implicitly or explicitly), $L(x, y, \theta)$ be the loss function used by the DNN, and θ be a set of parameters which is to be optimized over D_{train} for the DNN. For simplicity, $L(x, y, \theta)$ could be written in short as $L(x, \theta)$ or even $L(x)$, so do some other similar notations. Moreover, we assume in this paper that the last layer of the DNN be a softmax layer, but it should be noted that other functions can also be used.

Adversarial Training with the l_2 Norm Constraint

The adversarial training method with the l_2 norm constraint (AT) is a supervised method, which attempts to find the worst perturbed example in the neighborhood of a natural example to mislead the classification. Such perturbed examples are then augmented into the training set for training a better DNN. The objective of this adversarial training method can be written as:

$$\min_{\theta} \max_{x \in B(x_0, \epsilon)} L(x, y, \theta), \tag{1}$$

where x indicates the perturbed version of a natural example x_0 (with the label y) within a small neighborhood $B(x_0, \epsilon)$ (which is defined by $\|x - x_0\|_2 \leq \epsilon$).

Virtual Adversarial Training

Different from the adversarial training method with the l_2 norm constraint (AT), Virtual Adversarial Training (VAT) does not require the label information. It tends to find the worst perturbed example near a natural example so that the output of DNN $f(x, \theta)$ can be altered. The corresponding objective is defined as:

$$\min_{\theta} \max_{x \in B(x_0, \epsilon)} D(f(x_0, \theta), f(x, \theta)), \tag{2}$$

where $D(f(x_0, \theta), f(x, \theta))$ denotes the divergence between the outputs $f(x_0, \theta)$ and $f(x, \theta)$. For simplicity, $D(f(x_0, \theta), f(x, \theta))$ is defined in this paper as the Euclidean distance between the outputs, i.e., $\|f(x_0, \theta) - f(x, \theta)\|_2$, but it is straightforward to extend the Euclidean distance to other divergence measures.

Main Methodology

We first present a reasonable assumption.

Assumption 1: Given a sensible loss function $L(x, y, \theta) : R^I \rightarrow R$ for a specific learning task, we assume that, there exists a small threshold σ_{th}, such that those inputs x satisfying $L(x, y, \theta) \leq \sigma_{th}$ can be correctly classified.

Note that such an assumption generally holds for common loss functions such as the cross entropy and the square error. A detailed analysis on the assumption can be seen in the appendix of the supplementary materials. With the above notations and assumptions, the adversarial training problem can be described as follows.

Problem Formulation: Assume that a natural example x_0 satisfies $L(x_0, y_0, \theta) \leq \sigma_1$ where $\sigma_1 << \sigma_{th}$, i.e., the example x_0 can be classified correctly with a high confidence. An adversarial example x_{ad} is then defined as the worst perturbed sample such that $L(x_{ad}, y_0, \theta) > \sigma_{th}$, i.e., x_{ad} will be mis-classified. The objective of adversarial training for a specific x_0 can be reformulated as

$$\min_{\theta} \max_{x \in B(x_0, \epsilon)} |L(x, y, \theta) - L(x_0, y, \theta)|.$$

Robustness Against Adversarial Examples

Before we interpret our robustness analysis against adversarial examples, we set out Lemma 0.1 as follows:

Lemma 0.1 *Given a natural example x_0 satisfying $L(x_0, y_0, \theta) \leq \sigma_1$ (where $0 \leq \sigma_1 << \sigma_{th}$), if $\forall x \in B(x_0, \epsilon)$, $\exists \sigma_2 : 0 \leq \sigma_2 \leq \sigma_{th} - \sigma_1$, it holds that*

$$|L(x, y_0, \theta) - L(x_0, y_0, \theta)| \leq \sigma_2 \ , \tag{3}$$

then, all the data points in $B(x_0, \epsilon)$ can be classified correctly.

The proof is provided in the appendix of the supplementary materials.

Lemma 0.1 states that, if the loss of data points nearby x_0 is sufficiently close to that of x_0, then all these data points can be classified correctly, since the natural example x_0 has been already classified correctly with a high confidence. In other words, whether the nearby points around x_0 can be classified correctly is affected by the stability of the loss function $L(x, y, \theta)$ in the region $B(x_0, \epsilon)$. We also say that $L(x, y, \theta)$ is robust in the region $B(x_0, \epsilon)$, and thus there exist no adversarial examples in this region, since all the data in this region are classified into the same category.

Remark. Previous research studies the adversarial examples mainly through considering whether the adversarial perturbation can guide the natural example to cross the classification boundary in a less rigorous way. Moreover, it would be difficult to investigate the shape of the classification boundary when data lie in a high dimensional space. In comparison, we consider in this paper the robustness against adversarial examples from the perspective of the loss function stability, which would lead to strict analysis as follows.

In order to describe the stability of $L(x, y, \theta)$ in the neighborhood of x, we propose the following novel energy function as given in Definition 0.6.

Definition 0.1 *Let $L : R^I \rightarrow R$ be a differential and integral function and $B(x_0, \epsilon)$ be a small neighborhood of x_0 with radius ϵ. Then, the energy of $L(x)$ in this neighborhood is defined as:*

$$E_B(\theta) = \int_B ||\nabla_x L(x, \theta)||_2 dV, \tag{4}$$

where V denotes the volume.

This energy describes a metric measuring the stability of a function, i.e., how a function would change within a small region defined by $B(x_0, \epsilon)$. More precisely, the integral of the l_2 norm of the gradient of the loss with respect to the input x measures how the loss function changes at each point in $B(x_0, \epsilon)$. Intuitively, if the variation on each point is not large, the loss function would not change dramatically in this neighborhood of each point. This means that the loss function would be more stable. Importantly, we will prove that minimizing such energy function can guarantee the robustness for adversarial examples in $B(x_0, \epsilon)$. Before that, we provide Lemma 0.2.

Lemma 0.2 *Let $B(x_0, \epsilon) \in \mathbb{R}^I$ be a small neighborhood of natural example x_0 with label y_0, and x be an arbitrary point within $B(x_0, \epsilon)$. If the value of energy $E_B(\theta) = \int_B \|\nabla_x L(x, \theta)\|_2 dV$ decreases, then the number of examples classified correctly in $B(x_0, \epsilon)$ increases. When the energy goes to zero, the number of adversarial examples in $B(x_0, \epsilon)$ goes to zero.*

Proof of Lemma 0.2 is provided in the appendix of the supplementary materials.

Lemma 0.2 shows that decreasing the energy function leads to increasing the number of points x such that $|L(x) - L(x_0)| \leq \sigma_{th}$ in $B(x_0, \epsilon)$. In other words, a more number of points in $B(x_0, \sigma)$ would be correctly classified according to Lemma 0.1. When the energy function is small enough, there would be no adversarial examples gradually. Therefore, this novel energy function can be used to measure the robustness against adversarial examples in $B(x_0, \epsilon)$.

New Insight to Traditional Adversarial Methods

In this subsection, using our proposed stability measure, we provide interpretations as well as new insight to the previous traditional adversarial training methods including both supervised and semi-supervised version (Adversarial Training with l_2 norm constraint and VAT). Moreover, we prove that these traditional adversarial training methods are just to minimize the lower bound of the proposed energy along the radius, which however leads to insufficient robustness against adversarial examples. Such disadvantages will be analyzed and we then propose a more rational and practical optimization method.

First, we set out Definition 0.2 to describe the notion of the energy function along the radius.

Definition 0.2 *Let the spherical coordinate of $x \in B(x_0, \epsilon)$ be (r, ϕ) where $r \in [0, \epsilon]$ and $\phi \in [-\pi, \pi]^{I-1}$. Then, the energy along radius on ϕ is defined by*

$$E_\epsilon(\phi) = \int_0^\epsilon ||\nabla_x L(r, \phi)||_2 dr. \tag{5}$$

The energy E_ϵ is defined in the spherical coordinate system and describes the total variation of the function $L(r, \phi)$ along the radius at angle ϕ. We present Lemma 0.3 for a further explanation.

Lemma 0.3 *Let $B(x_0, \epsilon) \in \mathbb{R}^I$ be a small neighborhood of natural example x_0 with label y_0 and $x_{ad} \in B(x_0, \epsilon)$ such that $|L(x_{ad}) - L(x_0)| \geq |L(x) - L(x_0)|$ for all $x \in B(x_0, \epsilon)$. Suppose that x_{ad} is on the boundary of $B(x_0, \epsilon_1)$ $(\epsilon_1 \leq \epsilon)$ and the spherical coordinate of point x_{ad} can be expressed by (ϵ_1, ϕ_1) where $\phi_1 \in [-\pi, \pi]^{I-1}$. Then, we have*

$$\int_0^\epsilon ||\nabla_x L(r, \phi_1)||_2 dr \geq |L(x_{ad}) - L(x_0)|. \tag{6}$$

(Proof is provided in the appendix of the supplementary materials).

It is easy to reformulate the adversarial training method with l_2 norm constraint (AT) as follows (Lyu, Huang, and Liang 2015):

$$\begin{aligned} \min_\theta \max_{x \in B(x_0, \epsilon)} |L(x, \theta) - L(x_0, \theta)| \\ = \min_\theta |L(x_{ad}, \theta) - L(x_0, \theta)|. \end{aligned} \tag{7}$$

Remark. If we compare Eq. (7) with inequality (6), it can be noted that this traditional adversarial training method with l_2 norm constraint (AT) is equivalent to minimizing the lower

bound of the energy $E_\epsilon(\phi_1)$.
Only when the adversarial example is on the boundary of $B(x_0, \epsilon)$ and the function $L(r, \phi_1)$ is monotonically increasing w.r.t r, the traditional adversarial training method can be equivalent to minimizing the energy E_ϵ itself. Unfortunately, it is surely not guaranteed that the adversarial example is always on the boundary and the function $L(r, \phi_1)$ always monotonically increases, when ϵ increases.

Similarly, we can also prove VAT is equivalent to minimizing a lower bound of the energy along the radius at a certain angle ϕ. Before the proof, we present Lemma 0.4.

Lemma 0.4 *Let $B(x_0, \epsilon) \in \mathbb{R}^I$ be a small neighborhood of natural example x_0 with label y_0 and $x_{va} \in B(x_0, \epsilon)$ such that $\|f(x_{va}) - f(x_0)\|_2 \geq \|f(x) - f(x_0)\|_2$ for all $x \in B(x_0, \epsilon)$. Suppose that x_{va} is on the boundary of $B(x_0, \epsilon_1)$ $(\epsilon_1 \leq \epsilon)$ and the spherical coordinate of point x_{va} can be expressed by (ϵ_1, ϕ_2) where $\phi_2 \in [-\pi, \pi]^{I-1}$. Then, we have*

$$\int_0^\epsilon ||\nabla_x f(r, \phi_2)||_2 dr \geq \|f(x_{va}) - f(x_0)\|_2 \tag{8}$$

(Proof is provided in the appendix of the supplementary materials).

On the other hand, we can readily reformulate the VAT as (**?**):

$$\min_\theta \max_{x \in B(x_0, \epsilon)} \|f(x, \theta) - f(x_0, \theta)\|_2 = \min_\theta \|f(x_{va}, \theta) - f(x_0, \theta)\|_2 \tag{9}$$

Remark. If we compare Eq. (9) with Inequality (33), it can be noted that VAT is equivalent to minimizing the lower bound of energy $E_\epsilon(\phi_2)$.

Similarly, only when the adversarial example is on the boundary of $B(x_0, \epsilon)$ and the function $f(r, \phi_2)$ monotonically increases, the VAT would be exactly equivalent to minimizing the energy $E_\epsilon(\phi_2)$.

In summary, although the previous adversarial training methods could achieve good performance on both natural examples and adversarial examples, there are some inherit drawbacks. Note that the traditional adversarial training methods minimize the lower bound of the energy function each iteration which can reduce the value of the energy function to some degree. However, it cannot ensure the value of energy small enough. Intuitively, the traditional methods just consider the worst point in $B(x_0, \epsilon)$ which cannot restrict the total variation in neighborhood of x_0. This may ignore some other potential risk points. To illustrate this, We show in Fig. 1 that, even when the risk of the worst point has been reduced, the traditional methods could not guarantee the robustness against adversarial examples.

In Fig. 1, the loss for the worst point x_{adv} in $B(x_0, \epsilon)$ has been reduced to a small enough value (below the risk threshold θ_{th}). However, there exists also a small region $R_1 \in B(x_0, \epsilon)$ (the region in blue circle) such that $|L(x) - L(x_0)| \geq \sigma_{th}$ where $x \in R_1$, which means the examples in region R_1 are not guaranteed to be classified correctly according to the assumption mentioned before. According

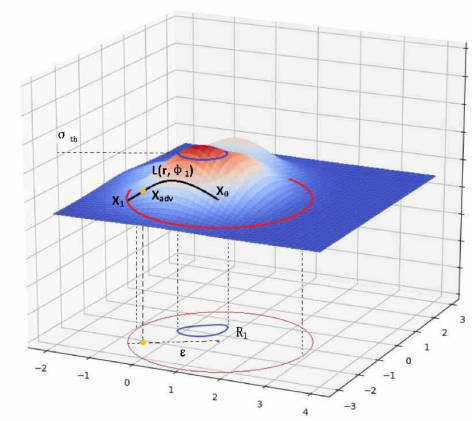

Figure 1: Illustration of the function $L(x)$ w.r.t input x where x is 2-dimensional. x_0 is a natural example and the red circle denotes its neighborhood $B(x_0, \epsilon)$. The region in the blue circle represents the risk region where the points cannot be guaranteed to be classified correctly $(L(x) \geq \sigma_{th})$. The black curve connecting x_0 and x_1 is the function $L(r, \phi)$ w.r.t r, and $E_\epsilon(r, \phi)$ is the corresponding energy.

to Fig. 1, for the traditional methods, minimizing $L(x_{ad})$ certainly cannot guarantee reducing the overall variations within all the nearby points as defined by the energy function given by Eq. (4). Therefore, there might exist other risk points. For tackling this problem, we additionally restrict the energy function (the total variation) within the neighborhood of natural example x_0. **Note that although the traditional methods minimize the loss function of different worst points for different iterations, sometimes finite points might be insufficient to guarantee the robustness. For our method, we additionally use the information of the first derivative to improve the stability (information of the first derivative might not solve the whole problem but alleviate it)**.

However, it is difficult to minimize the function of Eq. (4), since it requires the computation of integration. Instead, we propose in the following a more practical algorithm that is able to achieve the same objective. We first present Theorem 0.5.

Theorem 0.5 *Let $B(x_0, \epsilon) \in \mathbb{R}^I$ be a small neighborhood of natural example x_0 with label y_0 and x be an arbitrary point in $B(x_0, \epsilon)$. If the value of the energy $E_B(\theta) = \int_B \|\nabla_x L(x, \theta)\|_2 dV$ decreases, the value of the energy $E_\epsilon(\phi, \theta) = \int_0^\epsilon ||\nabla_x F(r, \phi, \theta)||_2 dr$ decreases almost everywhere in $[-\pi, \pi]^{I-1}$. When the energy $E_B(\theta)$ goes to zero, the energy $E_\epsilon(\phi, \theta)$ goes to zero almost everywhere in $[-\pi, \pi]^{I-1}$.*
(Proof is provided in the appendix of the supplementary materials.)

In the above, for a measurable set E, we say that a property holds **almost everywhere** on E, or it holds for almost all $x \in E$, provided there is a subset E_0 of E for which $m(E_0) = 0$ ($m(E_0)$ denotes the measure for E_0 and the property holds for all $x \in E - E_0$.

Theorem 0.5 states that decreasing the total energy E_B can lead to a reduction of the energy along the radius E_ϵ. Therefore, we can reduce all of E_ϵ by penalizing the total energy E_B. This naturally leads to a new method to enrich the traditional adversarial methods with energy regularization. We describe this new method as follows.

$$\min_{\theta} \max_{x} L(x, \theta) + \lambda \min_{\theta} \int_B ||\nabla_x L(x, y, \theta)||_2 dV. \quad (10)$$

In (10), the second term presents the energy regularization which is defined by the energy E_B, and λ is a positive trade-off hyper-parameter. Again, the energy function describes the overall variation of $L(x)$ in the neighborhood, which is significantly distinguished from those traditional methods acting merely on a single point. According to Lemma 0.2 and Theorem 0.5, reducing the energy E_B leads to decreasing the number of adversarial examples as well as the energy E_ϵ. Intuitively, penalizing the total variations of the function $L(x, y, \theta)$ can help avoid the dramatic fluctuation of the loss function as illustrated in Fig. 1.

However, the optimization problem (10) is again impractical since the second term requires integration. For convenient optimization, we change the second term with $\max_{x\in B} ||\nabla_x L(x, y, \theta)||_2$ which is closely related to the upper bound of E_B and E_ϵ in the sense that minimizing the term is equivalent to minimizing the upper bound of E_B and E_ϵ:

$$\min_{\theta} \max_{x\in B} L(x, \theta) + \lambda \max_{x\in B} ||\nabla_x L(x, y, \theta)||_2. \quad (11)$$

This new regularization can also be extended to VAT:

$$\begin{aligned} \min_{\theta} \max_{x\in B} & D(f(x_i, \theta), f(x_i + \epsilon_{vat}, \theta)) \\ & + \lambda \max_{x\in B} ||\nabla_x f(x, \theta)||_2. \end{aligned} \quad (12)$$

Again, our proposed method is equivalent to decreasing both the lower bound and upper bound of energy E_ϵ. Relevant proof and details can be seen in the appendix of the supplementary materials.

Practical Optimization Algorithm

We design practical optimization algorithms for our proposed new framework, which basically extends the previous methods with the novel energy regularization. For convenience, we start with the problem (11), while the problem (12) can be solved in a similar way. In the problem (11), the first term can be solved with the traditional adversarial training method. The second term can be divided into two problems: inner maximization problem and outer minimization problem. However, for the inner problem, since $\|\nabla_x L(x, y, \theta)\|_2$ is a non-convex function, it is difficult to evaluate the maximizer of function $\|\nabla_x L(x, y, \theta)\|_2$. Following many similar approaches (Lyu, Huang, and Liang 2015), we relax it to the convex problem with the first order Taylor expansions:

$$\begin{aligned} \max_{x\in B(x_0,\epsilon)} & ||\nabla_x L(x_0, y_0, \theta)||_2 \\ & + \nabla_x \|\nabla_x L(x_0, y_0, \theta)\|_2^T (x - x_0). \end{aligned} \quad (13)$$

The problem (34) is now a convex problem w.r.t x and can be solved by Lagrangian multiplier method. The maximizer can be calculated as:

$$x_{max} = \epsilon \overline{\nabla_x \|\nabla_x L(x_0, y_0, \theta)\|_2} + x_0, \quad (14)$$

where $\bar{\cdot}$ represents the normalized operator. The gradient of $\|\nabla_x L(x_0, y_0, \theta)\|_2$ w.r.t x is difficult to compute. We can use the finite difference method to approximate it:

$$\begin{aligned} x_{max} &= \epsilon \overline{\nabla_x \|\nabla_x L(x_0, y_0, \theta)\|_2} + x_0 \\ &= \epsilon \overline{H(x_0) \nabla_x L(x_0)} + x_0 \\ &\approx \epsilon \overline{\frac{\nabla_x L(x_0 + \xi \nabla_x L(x_0)) - \nabla_x L(x_0)}{\xi}} + x_0, \end{aligned} \quad (15)$$

where ξ is a small value. In this paper, we set $\xi = 10^{-6}$. More details of derivation of (37) are provided in the appendix. After computing the maximizer x_{max} of inner problem, the outer problem can be solved by the gradient decent method. The whole algorithm of Adversarial Training with Energy Regularization we called in short ATER is shown in Algorithm 1. We also develop the VAT with Energy Regularization (in short VATER) which is put in the appendix of the supplementary materials.

Algorithm 1 Algorithm for ATER.

for number of training iterations **do**
  Sample a batch of labeled data (x_i, y_i) with size N.
  for i in 1...N **do**
    $d_i^a \leftarrow \overline{\nabla_x \mathcal{L}(y_i, x_i, \theta)}$
    $\epsilon_{adv}^i = \xi d_i^a$
    $d_i^e \leftarrow \overline{\frac{\nabla_x L(x_i + \xi \nabla_x f(x_i)) - \nabla_x L(x_i)}{\xi}}$
    $x_{max}^i = \epsilon d_i^e + x_i$
  end for
  Update the parameters of neural network with stochastic gradient:
  $-\nabla_\theta \frac{1}{N} \sum_{i=1}^N log\mathcal{L}(y_i, x_i, \theta) - \nabla_\theta \frac{1}{N} \sum_{i=1}^N log\mathcal{L}(y_i, x_i + \epsilon_{adv}^i, \theta) - \nabla_x \frac{1}{N} \sum_{i=1}^N \|\nabla_\theta L(x_{max}^i, y_i, \theta)\|_2$
end for

Experiments

We evaluate the effectiveness of our proposed methods including Adversarial Training with Energy Regularization (ATER) and Virtual Adversarial Training with Energy Regularization (VATER) on datasets MNIST, CIFAR-10 for supervised tasks and we exploit SVHN additionally for semi-supervised tasks following the experimental setting used in the most related work (Miyato et al. 2018). Specifically, for MNIST, we apply the conventional fully connected neural network with the same setting as (Miyato et al. 2018). The number of units in the hidden layers are set to $\{1, 200, 600, 300, 150\}$ and the activate function is relu with batch normalization for each layer. We have conducted the experiments for the proposed ATER and VATER

in comparison with the baseline model and various traditional adversarial training methods. For the hyper parameter λ in (11) and (12), we simply set it to 0.1 empirically. For CIFAR-10 and SVHN, we utilize the structure called 'conv-large' following (Miyato et al. 2018). We use the $50,000$ labeled samples of CIFAR-10 to train this model and test with $10,000$ samples for the supervised task. For these two datasets the hyper-parameter λ is set to 0.5. Note that the best hyper-parameters are chosen from $\{0.1, 0.2, 0.5, 0.7, 1.0\}$ empirically.

Method	MNIST
SVM	1.40
Dropout (Srivastava et al. 2014)	1.05
Ladder networks (Rasmus et al. 2015)	$0.57(\pm 0.02)$
Adversarial, L_∞ norm constraint (Goodfellow, Shlens, and Szegedy 2014)	$0.78(\pm 0.03)$
Adversarial, L_2 norm constraint (Miyato et al. 2017)	$0.71(\pm 0.03)$
RPT (Miyato et al. 2017)	0.82
Baseline	$1.11(\pm 0.06)$
VAT	$0.64(\pm 0.05)$
ATER	$0.57(\pm 0.03)$
VATER	**0.55**($\pm$ 0.02)

Table 1: Test error rate (%) on MNIST in supervised learning

Method	CIFAR-10
Network in Network (Lin, Chen, and Yan 2013)	8.81
All-CNN (Springenberg et al. 2014)	7.25
Deeply Supervised Net (Lee et al. 2015)	7.97
Highway Network (Srivastava, Greff, and Schmidhuber 2015)	7.72
RPT (Miyato et al. 2017)	6.25 ± 0.04
ResNet (1,001 layers) (He et al. 2016)	4.62 ± 0.2
DenseNet (190 layers) (Huang et al. 2017)	**3.46**
Baseline	6.76 ± 0.07
VAT	5.81 ± 0.05
Baseline+l_2 adversarial	5.82 ± 0.04
ATER	5.43 ± 0.05
VATER	5.20 ± 0.05

Table 2: Test error rate % on CIFAR-10 in supervised learning

Table 1-2 show the results of different models on MNIST and CIFAR-10 respectively for the supervised task. Without tuning the parameter λ, our proposed methods already achieve the best performance on MNIST dataset over all the other algorithms. On CIFAR-10, our proposed adversarial method VATER performs the best among all the adversarial methods, but worse than the DenseNet and ResNet, which exploit a much deeper architecture. In future, we can also apply our method on such deeper structures to investigate if further improvements can be obtained.

To further examine if the proposed methods can be more robust to the adversarial examples, we generate in the test datasets of MNIST and CIFAR-10 10,000 adversarial examples according to FSGM and 2-norm attacks (Lyu, Huang, and Liang 2015) respectively. We increase the level of adversarial noise gradually from 0 to 8 in MNIST (with the step size as 1) and from 0 to 13 in CIFAR-10 (with the step size as 1.6). We then test the performance of various methods on these adversarial examples. The performance is plotted in Fig. 2. As clearly observed, the proposed VATER and ATER show much better robustness against two types of adversarial examples. Particularly, when the adversarial noises are small, all the adversarial training methods show similar results but perform much better than the CNN (exploiting no adversarial training); when the adversarial noises are heavier, the proposed VATER and ATER demonstrate clearly better performance, verifying their significant robustness.

In summary, for all the experiments, our proposed methods achieve superior performance than all the traditional adversarial training methods. We attribute this success to the additionally penalizing of the upper bound of the energy function that can reduce the overall variation in the neighborhood $B(x_0, \epsilon)$. In comparison, the traditional adversarial methods just consider to reduce the loss for the adversarial examples. Moreover, the experiments indicate that the first derivative of the loss $L(x)$ w.r.t input x can provide more information.

Table 3: Test performance on SVHN in semi-supervised learning

Method	SVHN (1,000 labeled) Test error rate(%)
SWWAE (Zhao et al.)	23.56
Skip Generative Model (Maaløe et al. 2016)	16.30
GAN with feature matching (Salimans et al. 2016)	8.11
Π model (Laine and Aila 2016)	5.43
RPT (Miyato et al. 2017)	$8.41(\pm 0.24)$
VAT	$5.77(\pm 0.32)$
VATER	**4.92**($\pm$0.10)

Table 4: Test performance on CIFAR-10 in semi-supervised learning

Method	CIFAR-10 (4,000 labeled) Test error rate(%)
Ladder networks, Γ model (Rasmus et al. 2015)	20.40
CatGAN (Springenberg 2015)	19.58
GAN with feature matching (Salimans et al. 2016)	18.63
Π model (Laine and Aila 2016)	16.55
RPT (Miyato et al. 2017)	$18.56(\pm 0.29)$
VAT	$14.82(\pm 0.38)$
VATER	**12.53**($\pm$0.23)

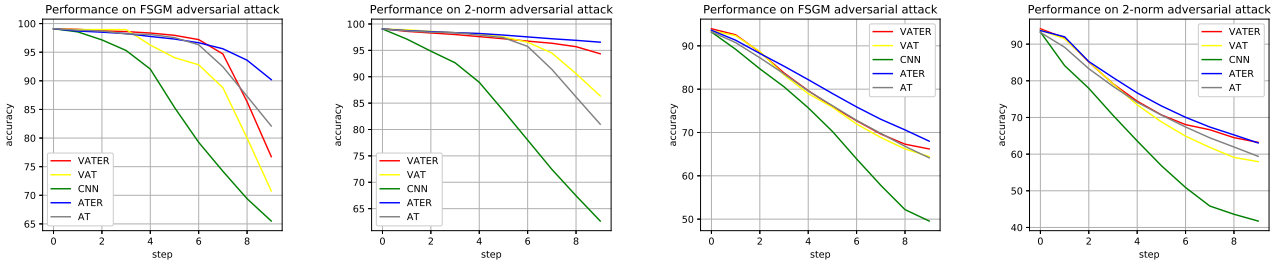

(a) FSGM attack in MNIST (b) l_2 attack in MNIST (c) FSGM attack in CIFAR-10 (d) l_2 attack in CIFAR-10

Figure 2: Performance of various methods on different adversarial attacks. VATER and ATER show the best robustness. Better viewed in color.

Table 3-4 demonstrate the results of different models on SVHN and CIFAR-10 for semi-supervised learning. For the semi-supervised task, we just apply our proposed method VATER since it is an unsupervised adversarial training method. As observed, our model again attains the best performance on both the two datasets.

Taking the example of CIFAR-10, we evaluate the convergence performance of our proposed models as well as their robustness against adversarial examples generated by AT. Both the evaluations are based on the supervised setting.

We plot the convergence curves for our proposed methods in Figure 3. Particularly, the figure shows the error rate for the different methods on both the training set and test set. The red lines indicate the convergence curves for our proposed methods (VATER and ATER) on the test set. The blue ones present the curves of the traditional adversarial training methods (VAT and AT). Although the training curves are similar, our proposed methods attain better convergence than their traditional counterparts on the test set.

Conclusion

In this paper, we investigate the model robustness against adversarial examples from the perspective of function stability. We develop a novel energy function to describe the stability in the small neighborhood of natural examples and prove that reducing such energy can guarantee the robustness for adversarial examples. We also offer new insights to traditional adversarial methods (AT and VAT) showing that such traditional methods merely decrease certain lower bounds of the energy function. We analyze the disadvantage of the traditional methods and propose accordingly more rational methods to minimize both the upper bound and lower bound of the energy function. We implement our methods on both supervised and semi-supervised tasks and achieve superior performance on benchmark datasets.

References

[Cisse et al. 2017] Cisse, M.; Bojanowski, P.; Grave, E.; Dauphin, Y.; and Usunier, N. 2017. Parseval networks: Improving robustness to adversarial examples. *arXiv preprint arXiv:1704.08847*.

[Fawzi, Fawzi, and Frossard 2018] Fawzi, A.; Fawzi, O.; and Frossard, P. 2018. Analysis of classifiers' robustness to adversarial perturbations. *Machine Learning* 107(3):481–508.

[Fawzi, Moosavi-Dezfooli, and Frossard 2016] Fawzi, A.; Moosavi-Dezfooli, S.-M.; and Frossard, P. 2016. Robustness of classifiers: from adversarial to random noise. In *Advances in Neural Information Processing Systems*, 1632–1640.

[Finlay, Oberman, and Abbasi 2018] Finlay, C.; Oberman, A.; and Abbasi, B. 2018. Improved robustness to adversarial examples using lipschitz regularization of the loss. *arXiv preprint arXiv:1810.00953*.

[Goodfellow, Shlens, and Szegedy 2014] Goodfellow, I. J.; Shlens, J.; and Szegedy, C. 2014. Explaining and harnessing adversarial examples. *arXiv preprint arXiv:1412.6572*.

[He et al. 2016] He, K.; Zhang, X.; Ren, S.; and Sun, J. 2016. Identity mappings in deep residual networks. In *European conference on computer vision*, 630–645. Springer.

[He et al. 2017] He, K.; Gkioxari, G.; Dollár, P.; and Girshick, R. 2017. Mask r-cnn. In *Computer Vision (ICCV), 2017 IEEE International Conference on*, 2980–2988. IEEE.

[Huang et al. 2017] Huang, G.; Liu, Z.; Van Der Maaten, L.; and Weinberger, K. Q. 2017. Densely connected convolutional networks. In *CVPR*, volume 1, 3.

[Kos, Fischer, and Song 2018] Kos, J.; Fischer, I.; and Song, D. 2018. Adversarial examples for generative models. In *2018 IEEE Security and Privacy Workshops (SPW)*, 36–42. IEEE.

[Kurakin, Goodfellow, and Bengio 2016] Kurakin, A.; Goodfellow, I.; and Bengio, S. 2016. Adversarial machine learning at scale. *arXiv preprint arXiv:1611.01236*.

[Laine and Aila 2016] Laine, S., and Aila, T. 2016. Temporal ensembling for semi-supervised learning. *arXiv preprint arXiv:1610.02242*.

[LeCun, Bengio, and Hinton 2015] LeCun, Y.; Bengio, Y.; and Hinton, G. 2015. Deep learning. *nature* 521(7553):436.

[Lee et al. 2015] Lee, C.-Y.; Xie, S.; Gallagher, P.; Zhang, Z.; and Tu, Z. 2015. Deeply-supervised nets. In *Artificial Intelligence and Statistics*, 562–570.

[Lin, Chen, and Yan 2013] Lin, M.; Chen, Q.; and Yan, S. 2013. Network in network. *arXiv preprint arXiv:1312.4400*.

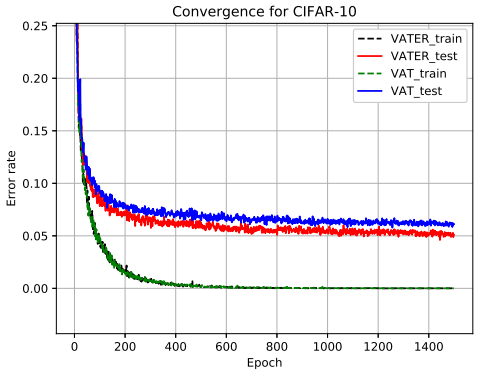

(a) Convergence for VATER and VAT on CIFAR-10

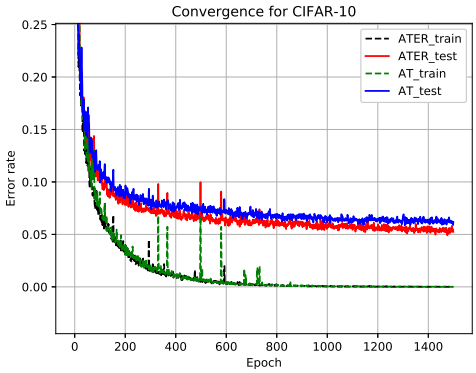

(b) Convergence for ATER and AT on CIFAR-10

Figure 3: The figure shows the error rate for different methods on both the training set and the test set. Although the training curves are similar, our proposed methods attain better convergence than their traditional counterpart on the test set.

[Liu and Nocedal 1989] Liu, D. C., and Nocedal, J. 1989. On the limited memory bfgs method for large scale optimization. *Mathematical programming* 45(1-3):503–528.

[Lyu, Huang, and Liang 2015] Lyu, C.; Huang, K.; and Liang, H.-N. 2015. A unified gradient regularization family for adversarial examples. In *Data Mining (ICDM), 2015 IEEE International Conference on*, 301–309. IEEE.

[Ma et al. 2018] Ma, X.; Li, B.; Wang, Y.; Erfani, S. M.; Wijewickrema, S.; Houle, M. E.; Schoenebeck, G.; Song, D.; and Bailey, J. 2018. Characterizing adversarial subspaces using local intrinsic dimensionality. *arXiv preprint arXiv:1801.02613*.

[Maaløe et al. 2016] Maaløe, L.; Sønderby, C. K.; Sønderby, S. K.; and Winther, O. 2016. Auxiliary deep generative models. *arXiv preprint arXiv:1602.05473*.

[Miyato et al. 2015] Miyato, T.; Maeda, S.-i.; Koyama, M.; Nakae, K.; and Ishii, S. 2015. Distributional smoothing with virtual adversarial training. *arXiv preprint arXiv:1507.00677*.

[Miyato et al. 2017] Miyato, T.; Maeda, S.-i.; Koyama, M.; and Ishii, S. 2017. Virtual adversarial training: a regularization method for supervised and semi-supervised learning. *arXiv preprint arXiv:1704.03976*.

[Miyato et al. 2018] Miyato, T.; Maeda, S.-i.; Ishii, S.; and Koyama, M. 2018. Virtual adversarial training: a regularization method for supervised and semi-supervised learning. *IEEE transactions on pattern analysis and machine intelligence*.

[Papernot, McDaniel, and Goodfellow 2016] Papernot, N.; McDaniel, P.; and Goodfellow, I. 2016. Transferability in machine learning: from phenomena to black-box attacks using adversarial samples. *arXiv preprint arXiv:1605.07277*.

[Rasmus et al. 2015] Rasmus, A.; Berglund, M.; Honkala, M.; Valpola, H.; and Raiko, T. 2015. Semi-supervised learning with ladder networks. In *Advances in Neural Information Processing Systems*, 3546–3554.

[Salimans et al. 2016] Salimans, T.; Goodfellow, I.; Zaremba, W.; Cheung, V.; Radford, A.; and Chen, X. 2016. Improved techniques for training gans. In *Advances in Neural Information Processing Systems*, 2234–2242.

[Shaham, Yamada, and Negahban 2015] Shaham, U.; Yamada, Y.; and Negahban, S. 2015. Understanding adversarial training: Increasing local stability of neural nets through robust optimization. *arXiv preprint arXiv:1511.05432*.

[Springenberg et al. 2014] Springenberg, J. T.; Dosovitskiy, A.; Brox, T.; and Riedmiller, M. 2014. Striving for simplicity: The all convolutional net. *arXiv preprint arXiv:1412.6806*.

[Springenberg 2015] Springenberg, J. T. 2015. Unsupervised and semi-supervised learning with categorical generative adversarial networks. *arXiv preprint arXiv:1511.06390*.

[Srivastava et al. 2014] Srivastava, N.; Hinton, G.; Krizhevsky, A.; Sutskever, I.; and Salakhutdinov, R. 2014. Dropout: A simple way to prevent neural networks from overfitting. *The Journal of Machine Learning Research* 15(1):1929–1958.

[Srivastava, Greff, and Schmidhuber 2015] Srivastava, R. K.; Greff, K.; and Schmidhuber, J. 2015. Highway networks. *arXiv preprint arXiv:1505.00387*.

[Xu, Evans, and Qi 2017] Xu, W.; Evans, D.; and Qi, Y. 2017. Feature squeezing: Detecting adversarial examples in deep neural networks. *arXiv preprint arXiv:1704.01155*.

[Zhao et al.] Zhao, J.; Mathieu, M.; Goroshin, R.; and Lecun, Y. Stacked what-where auto-encoders. arxiv 2015. *arXiv preprint arXiv:1506.02351*.

Appendix

Analysis for Assumption 1 in Section 3.1

In this section, we prove that for common loss functions (e.g., cross entropy and square error) we can find a small constant σ_{th} such that if $L(x, y, \theta) < \sigma_{th}$, then the input x can be classified correctly. In this paper, we assume the last layer the softmax layer, then we have $\sum_i y_i = 1$ and $y_i \in [0, 1]$.

Cross Entropy Loss

The cross entropy loss is defined as $L_{ce} = -\sum_i l_i log(y_i)$ where $l = \{l_i\}_{i=1}^{O}$ (O is the output dimension) is an one hot label vector for input x_1. We assume $l_a = 1$ and others are zeros which means x belongs to class a. Then, we can reformulate the cross entropy loss as $L_{ce} = -logy_a$. If $L_{ce}(x_1, l) < \sigma_{th}$ for all $0 < \sigma_{th} < -log0.5$, x_1 can be classified correctly.

Proof:

$$L_{ce} < \sigma_{th} < -log0.5 \tag{16}$$

then we have

$$\begin{aligned} -logy_a &< \sigma_{th} < -log0.5 \\ \Rightarrow y_a &> e^{-\sigma_{th}} > 0.5 \end{aligned} \tag{17}$$

Since $\sum_i y_i = 1$ and $y_a > e^{-\sigma_{th}} > 0.5$, x_1 can be classified correctly.

Square Error Loss

The square error loss can be formulated as $L_{se} = \sum_i (y_i - l_i)^2$. Similarly, for the square error loss L_{se}, If $L_{se}(x_1, l) < \sigma_{th}$ for all $\sigma_{th} < 0.25$, x_1 can be classified correctly.

Proof:

$$\sum_i (y_i - l_i)^2 < \sigma_{th} \tag{18}$$

Since $l_a = 1$ and others are zeros, then we have

$$\begin{aligned} &\sum_{i/a} (y_i)^2 + (y_a - 1)^2 < \sigma_{th} \\ &\Rightarrow (y_a - 1)^2 < \sigma_{th} < 0.25 \\ &\Rightarrow y_a > \sigma_{th} > 0.5 \end{aligned} \tag{19}$$

Since $\sum_i y_i = 1$ and $y_a > 1 - \sqrt{\sigma_{th}} > 0.5$, x_1 can be classified correctly.

Proof for Lemmas

In this section, we prove the lemmas in the main paper. For convenience, we first set out some Theorem and Lemma.

Theorem 0.6 *Let $B \in \mathbb{R}^n$ and $f : \mathbb{R}^n \to \mathbb{R}$ and $g : \mathbb{R}^n \to \mathbb{R}$ are integrable and continues functions, then there exists a constant c such that*

$$\int_B f(x)g(x)dV = c \int_B g(x)dV \tag{20}$$

where V is the volume and $\int_B g(x)dV \neq 0$.

Proof:

We can directly find constant c:

$$\frac{\int_B f(x)g(x)dV}{\int_B g(x)dV} = c \tag{21}$$

Lemma 1. Let us define $g : \mathbb{R}^m \to \mathbb{R}$ by $g(\theta) = \int_B f(x, \theta)dV$ where $f : \mathbb{R}^I \to \mathbb{R}$ is differential and integrable. Then, if $g(\theta)$ decreases and goes to zero, $f(x, \theta)$ decreases and goes to zero almost everywhere in B.

(Def. For a measurable set E, we say that a property holds **almost everywhere** on E, or it holds for almost all $x \in E$, provided there is a subset E_0 of E for which $m(E_0) = 0$ ($m(E_0)$ denotes the measure for E_0) and the property holds for all $x \in E - E_0$).

Proof:

Let $N_0 = \{x | f(x) \geq n_0\}$ where n_0 is a sufficiently small value.

$$\begin{aligned} g(\theta) &= \int_B f(x, \theta)dV \\ &= \int_{N_0} f(x, \theta)dV + \int_{B-N_0} f(x, \theta)dV \\ &\geq \int_{N_0} f(x, \theta)dV \end{aligned} \tag{22}$$

When $g(\theta)$ decreases and goes to zero, $\int_{N_0} f(x, \theta)dV$ decreases and goes to zero. Then the measure of N_0 ($m(\{x | f(x) \geq n_0\})$) decreases and goes to zero which means the measure of $B - N_0$ (m($\{x | f(x) < n_0\}$)) increases and goes to $m(B)$. Therefore, $f(x, \theta)$ decreases and goes to zero almost everywhere in B.

Proof for Lemma 3.1

Lemma 3.1. Given a natural example x_0 satisfying $L(x_0, y_0, \theta) \leq \sigma_1$ (where $0 \leq \sigma_1 << \sigma_{th}$), if $\forall x \in B(x_0, \epsilon)$, $\exists \sigma_2 : 0 \leq \sigma_2 \leq \sigma_{th} - \sigma_1$, it holds that

$$|L(x, y_0, \theta) - L(x_0, y_0, \theta)| \leq \sigma_2 \ , \tag{23}$$

then, all the data points in $B(x_0, \epsilon)$ can be classified correctly.

Proof:

In this paper, we have proved in the previous section that there exists a σ_{th} such that if $L(x, y, \theta) \leq \sigma_{th}$, x can be classified correctly. Additionally, we assume that the natural examples can be classified correctly with a high confidence ($L(x_0, y_0, \theta) \leq \sigma_1 << \sigma_{th}$). Then, if $L(x, y_0, \theta) < L(x_0, y_0, \theta)$,

$$L(x, y_0, \theta) < \sigma_1 < \sigma_{th} \tag{24}$$

which means x can be classified correctly.

If $L(x, y_0, \theta) > L(x_0, y_0, \theta)$

$$\begin{aligned} |L(x, y_0, \theta) - L(x_0, y_0, \theta)| &= L(x_0, y_0, \theta) - L(x_0, y_0, \theta) \\ &< \sigma_2 < \sigma_{th} - \sigma_1 \\ \Rightarrow L(x_0, y_0, \theta) &< L(x_0, y_0, \theta) + \sigma_2 < \sigma_{th} \end{aligned} \tag{25}$$

Therefore, if $|L(x_0, y_0, \theta) - L(x_0, y_0, \theta)| \leq \sigma_2$, x_0 can be classified correctly.

Proof for Lemma 3.3 and Lemma 3.4

Here, we just prove Lemma 3.4 since Lemma 3.3 is a special case of Lemma 3.4.

Lemma 3.4. Let $B(x_0, \epsilon) \in \mathbb{R}^I$ be a small neighborhood of natural example x_0 with label y_0 and $x_{va} \in B(x_0, \epsilon)$ such that $\|f(x_{va}) - f(x_0)\|_2 \geq \|f(x) - f(x_0)\|_2$ for all $x \in B(x_0, \epsilon)$. Suppose that x_{va} is on the boundary of $B(x_0, \epsilon_1)$ ($\epsilon_1 \leq \epsilon$) and the spherical coordinate of point x_{va} can be expressed by (ϵ_1, ϕ_2) where $\phi_2 \in [-\pi, \pi]^{I-1}$. Then, we have

$$\int_0^{\epsilon} ||\nabla_x f(r, \phi_2)||_2 dr \geq \|f(x_{va}) - f(x_0)\|_2 \tag{26}$$

Proof:

$$\begin{aligned}\int_0^{\epsilon} ||\nabla_x f(r, \phi_2)||_2 dr &\geq \int_0^{\epsilon_1} ||\nabla_x f(r, \phi_2)||_2 dr \\ &\geq \int_0^{\epsilon_1} ||\nabla_x f(r, \phi_2) \cdot \overrightarrow{d}||_2 dr \\ &\geq || \int_0^{\epsilon_1} \nabla_x f(r, \phi_2) \cdot \overrightarrow{d}\, dr||_2 \\ &= \|f(x_{va}) - f(x_0)\|_2\end{aligned} \tag{27}$$

where, $\overrightarrow{d}$ is the unit vector pointing from x_0 to x_{va}. In the same way, we can prove Lemma 3.3.

Proof for Lemma 3.2

Lemma 3.2. Let $B(x_0, \epsilon) \in \mathbb{R}^I$ be a small neighborhood of natural example x_0 with label y_0 and x_{ar} be arbitrary point in $B(x_0, \epsilon)$. If the value of energy $E_B(\theta) = \int_B \|\nabla_x L(x, \theta)\|_2 dV$ decreases, the number of examples classified correctly in $B(x_0, \epsilon)$ increases. When the energy goes to zero, the number of adversarial examples in $B(x_0, \epsilon)$ goes to zero.

Proof:

we reformulate the energy in spherical coordinate:

$$\begin{aligned}E_B &= \int_B ||\nabla_x L(x)||_2 dV \\ &= \int_{S^{I-1}} \int_0^{\epsilon} ||\nabla_x L(r, \phi)||_2 r^{I-1} dr d\phi\end{aligned} \tag{28}$$

According to Theorem 2.1, there exists a constant r_1 such that

$$\begin{aligned}&\int_B ||\nabla_x L(r,\phi)||_2 dV \\ &\qquad = r_1 \int_{S^{I-1}} \int_0^{\epsilon} ||\nabla_x L(r, \phi)||_2 dr d\phi\end{aligned} \tag{29}$$

According to Lemma 3.4, we have

$$\begin{aligned}&r_1 \int_{S^{I-1}} \int_0^{\epsilon} ||\nabla_x L(r, \phi)||_2 dr d\phi \\ &\qquad \geq r_1 \int_{S^{I-1}} |L(\epsilon_1, \phi) - L(x_0)| d\phi\end{aligned} \tag{30}$$

where $\epsilon_1 \leq \epsilon$ and (ϵ_1, ϕ) is the spherical coordinate of arbitrary point x. Since E_B is the upper bound of $\int_{S^{I-1}} |L(\epsilon_1, \phi) - L(x_0)| d\phi$, when E_B decreases and goes to zero, $\int_{S^{I-1}} |L(\epsilon_1, \phi) - L(x_0)| d\phi$ decreases and goes to zero. According to Lemma 1, for almost all $x_{ar} \in B$, $|L(x_{ar}) - L(x_0)|$ decreases and goes to zero which means the number of adversarial examples in B decreases and goes to zero (according to Lemma 3.1).

Proof for Theorem 3.5

Theorem 3.5. Let $B(x_0, \epsilon) \in \mathbb{R}^I$ be a small neighborhood of natural example x_0 with label y_0. and x_{ar} be arbitrary point in $B(x_0, \epsilon)$. If the value of energy $E_B(\theta) = \int_B \|\nabla_x L(x, \theta)\|_2 dV$ decreases, the value of energy $E_\epsilon(\phi, \theta) = \int_0^{\epsilon} ||\nabla_x F(r, \phi, \theta)||_2 dr$ decreases almost everywhere in $[-\pi, \pi]^{I-1}$. When the energy $E_B(\theta)$ goes to zero, the energy $E_\epsilon(\phi, \theta)$ goes to zero almost everywhere in $[-\pi, \pi]^{I-1}$.

Proof:

Similar to Lemma 3.2, there exists a constant r_1 such that

$$\begin{aligned}&\int_B ||\nabla_x L(r,\phi)||_2 dV \\ &\qquad = r_1 \int_{S^{I-1}} \int_0^{\epsilon} ||\nabla_x L(r, \phi)||_2 dr d\phi \\ &\qquad = r_1 \int_{S^{I-1}} E_\epsilon(\phi) d\phi\end{aligned} \tag{31}$$

According to Lemma 1, when $E_B(\theta)$ decreases and goes to zero, for almost all $\phi \in [-\pi, \pi]^{I-1}$, $E_\epsilon = \int_0^{\epsilon} ||\nabla_x F(r, \phi)||_2 dr$ deceases and goes to zero.

Details of Practical Algorithm

In this paper, we minimize both the upper bound and lower bound of energy E_ϵ. The algorithm to minimize the lower bound is the same as the traditional adversarial training. Here, we only give the relevant proof and algorithm for the upper bound of E_ϵ and E_B:

The upper bound for E_B:

$$\begin{aligned}E_B &= \int_B ||\nabla_x L(x)||_2 dV \\ &\leq \int_B \max_{x \in B} \|\nabla L(x)\|_2 dV \\ &= \max_{x \in B} \|\nabla L(x)\|_2 \cdot Vol(B)\end{aligned} \tag{32}$$

The upper bound for E_ϵ:

$$\begin{aligned}E_\epsilon &= \int_0^{\epsilon} ||\nabla_x L(r, \phi)||_2 dr \\ &\leq \int_0^{\epsilon} \max_{x \in B} \|\nabla L(x)\|_2 dr \\ &= \max_{x \in B} \|\nabla L(x)\|_2 \cdot \epsilon\end{aligned} \tag{33}$$

Since $Vol(B)$ and ϵ are constants, reducing $\max_{x \in B} \|\nabla L(x)\|_2$ is equivalent to decreasing the upper bound of E_ϵ and E_B.

The problem (13) in the main paper can be reduced to:

$$\max_{\|r\|_p = \epsilon} \nabla_x \mathcal{F}^T r \tag{34}$$

where, $r = x - x_0$ and $\mathcal{F} = \|\nabla_x L(x_0, y_0, \theta)\|_2$. We solve it with the Lagrangian multiplier method and we have

$$\nabla_x \mathcal{F} r = \lambda(\|r\|_p - \epsilon)$$

Then we make the first derivative with respect to r:

$$\nabla_x \mathcal{F} = \lambda \frac{r^{p-1}}{p(\sum_i r_i^p)^{1-\frac{1}{p}}}$$

$$\nabla_x \mathcal{F} = \frac{\lambda}{p}(\frac{r}{\epsilon})^{p-1}$$

$$(\nabla_x \mathcal{F})^{\frac{p}{p-1}} = (\frac{\lambda}{p})^{\frac{p}{p-1}}(\frac{r}{\epsilon})^p \tag{35}$$

If we sum over two sides, we have

$$\sum (\nabla_x \mathcal{F})^{\frac{p}{p-1}} = \sum (\frac{\lambda}{p})^{\frac{p}{p-1}}(\frac{r}{\epsilon})^p$$

$$\|\nabla_x \mathcal{F}\|_{p^*}^{p^*} = (\frac{\lambda}{p})^{p^*} * 1$$

where p^* is the dual of p. $(\frac{1}{p} + \frac{1}{p^*} = 1)$

$$(\frac{\lambda}{p}) = \|\nabla_x \mathcal{F}\|_{p^*} \tag{36}$$

By combining (35) and (36), we have

$$r^* = \epsilon sign(\nabla \mathcal{F})(\frac{|\nabla \mathcal{F}|}{\|\nabla \mathcal{F}\|_{p^*}})^{\frac{1}{p-1}}$$

In this paper, $p = 2$, then we have

$$\begin{aligned} r^* &= \epsilon(\frac{\nabla \mathcal{F}}{\|\nabla \mathcal{F}\|_2}) \\ &= \epsilon \overline{\nabla_x \|\nabla_x L(x_0, y_0, \theta)\|_2} \end{aligned}$$

Therefore, the maximizer x_{max} can be calculated as:

$$x_{max} = r^* + x_0 = \epsilon \overline{\nabla_x \|\nabla_x L(x_0, y_0, \theta)\|_2} + x_0$$

$\nabla_x \|\nabla_x L(x_0, y_0, \theta)\|_2$ can be calculated as:

$$\begin{aligned} &\nabla_x \|\nabla_x L(x_0)\|_2 \\ &= [\frac{\partial \|\nabla_x L(x_0)\|_2^2}{\partial x_1}, \frac{\partial \|\nabla_x L(x_0)\|_2^2}{\partial x_2}, ..., \\ &\frac{\partial \|\nabla_x L(x_0)\|_2^2}{\partial x_I}] \cdot \frac{1}{2\|\nabla_x L(x_0)\|_2} \\ &= \frac{1}{\|\nabla_x L(x_0)\|_2}[\sum_{i=1}^{I} \frac{\partial \nabla_x L(x_0)}{\partial x_i}\frac{\partial \nabla_x L(x_0)}{\partial x_i \partial x_1}, \\ &\sum_{i=1}^{I} \frac{\partial \nabla_x L(x_0)}{\partial x_i}\frac{\partial \nabla_x L(x_0)}{\partial x_i \partial x_2}, ..., \\ &\sum_{i=1}^{I} \frac{\partial \nabla_x L(x_0)}{\partial x_i}\frac{\partial \nabla_x L(x_0)}{\partial x_i \partial x_I}] \\ &= \frac{1}{\|\nabla_x L(x_0)\|_2} \cdot H(x_0)\nabla_x L(x_0) \end{aligned}$$

Then, using the finite difference method, we have

$$\begin{aligned} &\frac{1}{\|\nabla_x L(x_0)\|_2} \cdot H(x_0)\nabla_x L(x_0) \\ &\approx \frac{1}{\|\nabla_x L(x_0)\|_2} \cdot \frac{\nabla_x L(x_0 + \xi \nabla_x L(x_0)) - \nabla_x L(x)}{\xi} \end{aligned}$$

where ξ is small value ($\xi = 10^{-6}$). Since $\frac{1}{\|\nabla_x L(x_0)\|_2}$ is scalar, we have

$$x_{max} \approx \epsilon \overline{\frac{\nabla_x L(x_0 + \xi \nabla_x L(x_0)) - \nabla_x L(x_0)}{\xi}} + x_0 \tag{37}$$

Algorithm for VATER

Algorithm 2 Algorithm for VATER.

for number of training iterations **do**
  Sample a batch of labeled data (x_l, y_l) with size N_l and a batch of unlabeled data (x_{ul}) with size N_{ul}. Z_{l_i} denotes the matrix of latent features of data with label i in a batch.
  for j in 1...n **do**
    $d \leftarrow \overline{\nabla_x D(f(x_i, \theta), f(x_i + r, \theta))|_{\epsilon=\xi d}}$
  end for
  $\epsilon_{vat} = \xi d$
  $d_i^e \leftarrow \frac{\nabla_x f(x_i + \xi \nabla_x f(x_i)) - \nabla_x f(x_i)}{\xi}$
  $x_{max}^i = \epsilon d_i^e + x_i$
  Update the parameters of neural network with stochastic gradient:

  $-\nabla_\theta \{\frac{1}{N}\sum_{i=1}^{N} L(x_i, y_i, \theta) - D(f(x_i, \theta), f(x_i + \epsilon_{vat}, \theta)) - \lambda \|\nabla_x f(x_{max}^i, \theta)\|_2\}$
end for